Electronic Transactions on Numerical Analysis.
Volume 65, pp. 372–386, 2026.

ISSN 1068–9613.
DOI: 10.1553/etna_vol65s372

ETNA
Kent State University and
Johann Radon Institute (RICAM)

AN OPERATIONAL JACOBI COLLOCATION FRAMEWORK FOR SOLVING LINEAR SYSTEMS OF DISTRIBUTED-ORDER FRACTIONAL DIFFERENTIAL EQUATIONS*

Z. SAKI† AND P. MOKHTARY†

Abstract. This paper introduces a novel collocation-based framework for the analysis and numerical solution of linear systems of distributed-order fractional differential equations (DOFDEs), formulated in the Caputo sense. Under suitable conditions we establish the analytic form of the exact solution and investigate its smoothness properties. The proposed numerical methodology is structured into two main steps. First, a high-order Gauss–Legendre quadrature rule is employed to accurately discretize the distributed-order integral, thereby reducing the original system to an equivalent multi-term fractional differential system. Second, an operational spectral collocation scheme is developed, based on a special family of generalized Jacobi polynomials as basis functions and Gauss–Legendre nodes as collocation points to further transform the problem into a well-structured block system of algebraic equations. A comprehensive convergence analysis is presented, demonstrating the spectral accuracy of the method. The efficiency of the proposed approach is validated through several illustrative examples, confirming its potential for solving complex fractional systems with distributed-order dynamics.

Key words. linear system of distributed-order fractional differential equations (DOFDEs), collocation method, generalized Jacobi polynomials, convergence analysis

AMS subject classifications. 26A33, 34A08, 39A33, 65D05, 37N30, 93C27

1. Introduction.

Fractional calculus has emerged as a powerful tool for modeling complex multi-scale phenomena characterized by memory, non-locality, and anomalous dynamics. These equations find applications across diverse fields, including non-Gaussian transport in turbulence [17, 18], non-Newtonian rheology [14, 27], and anomalous diffusion in porous media [3, 25]. This growing interest has motivated the development of various numerical techniques for fractional differential equations (FDEs), such as the variational iteration method [19], homotopy-based methods [15, 21], and spectral collocation methods [31].

Among the various extensions of classical fractional calculus, distributed-order fractional derivatives have gained particular attention. A distributed-order fractional derivative is defined as a fractional operator obtained by continuously integrating the differentiation orders across a prescribed range within a given domain. Distributed-order fractional differential equations (DOFDEs) thus constitute a natural generalization that subsumes both single-order and multi-term fractional differential equations as special cases. In recent decades, the application of DOFDEs has expanded considerably, enabling the precise modeling of diverse complex phenomena in fields such as optimal control [23], diffusion processes [12], and viscoelasticity [13]. Additional comprehensive discussions can be found in [20, 29, 30]. However, the inherent computational complexity of distributed-order fractional derivatives renders the derivation of exact analytical solutions for DOFDEs particularly challenging. Although a limited number of analytical solutions have been reported, they remain rare and often demand further exploration. Consequently, the development of robust and efficient numerical schemes for the accurate solution of DOFDEs remains a critical research priority.

In one of the earliest numerical investigations of DOFDEs, Diethelm and Ford [7] introduced a foundational two-stage framework. The first stage entails approximating the distributed-order derivative via a suitable quadrature rule, while the second involves applying

*Received October 4, 2025. Accepted June 9, 2026. Published online on August 17, 2026. Recommended by Mariarosa Mazza.
†Corresponding author: P. Mokhtary. Department of Mathematics, Faculty of Basic Sciences, Sahand University of Technology, Tabriz, Iran (mokhtary.payam@gmail.com).

ETNA
Kent State University and
Johann Radon Institute (RICAM)

an appropriate multi-term numerical scheme. Building upon this structure, subsequent studies have largely adhered to this two-stage methodology, differing primarily in their choice of discretization techniques for the second stage. Notable examples include numerical treatments of the distributed-order time-fractional diffusion equation [12], the distributed-order reaction-diffusion equation [16], the distributed-order diffusion equation using a reproducing kernel method [9], and the distributed-order time-fractional diffusion-wave equation employing a compact difference scheme [26]. Furthermore, various approaches have been developed, including methods based on the trapezoidal quadrature rule [4], finite difference schemes [10], the Gauss–Legendre quadrature method [28], the reproducing kernel method [11], radial basis function-based mesh-free methods [2], and the element-free Galerkin method [1].

Among the growing body of literature addressing DOFDEs, only a limited number of studies have focused on the numerical treatment of systems of such equations. Existing works on systems of DOFDEs have primarily concentrated on theoretical aspects, with little progress made in developing robust numerical methodologies. Consequently, the advancement of accurate and efficient numerical schemes for solving these systems represents a novel and valuable contribution to the field.

This paper details a numerical method specifically designed for solving distributed-order fractional differential equations (DOFDEs) of the form

$$\begin{cases} \displaystyle\int_0^m \omega(\nu) D^\nu U(t)\, d\nu = AU(t) + F(t), & t \in \Omega = [0,1], \\ U^{(j)}(0) = U_0^{(j)}, & j = 0, 1, \dots, m-1, \end{cases} \tag{1.1}$$

where the coefficient matrix is denoted by $A = [a_{ij}]_{i,j=1}^n \in \mathbb{R}^{n\times n}$, and the vector-valued source function is given by $F(t) = [f_j(t)]_{j=1}^n \in \mathbb{R}^n$, with each component $f_j \in L^1(\Omega)$. The vector $U(t) = [u_j(t)]_{j=1}^n \in \mathbb{R}^n$ represents the unknown solution, and $U_0^{(j)} = [u_{i,0}^{(j)}]_{i=1}^n \in \mathbb{R}^n$ denotes the vector of initial conditions. The fractional derivative is defined in the Caputo sense by [6]

$$D^\nu U(t) = I^{m-\nu} D^m U(t) = \frac{1}{\Gamma(m-\nu)} \int_0^t (t-\tau)^{m-\nu-1} U^{(m)}(\tau)\, d\tau,$$

where $\Gamma(\cdot)$ denotes the Gamma function and I^ν is the Riemann–Liouville fractional integral operator of order ν defined by

$$I^\nu U(t) = \frac{1}{\Gamma(\nu)} \int_0^t (t-\tau)^{\nu-1} U(\tau)\, d\tau.$$

Additionally, it is assumed that the weight function $\omega(\nu)$ is absolutely integrable over the interval $[0, m]$ and satisfies

$$\int_0^m \omega(\nu) s^\nu\, d\nu \neq 0 \qquad \text{for } \operatorname{Re}(s) > 0.$$

This study introduces a novel operational-based collocation framework for solving systems of DOFDEs (1.1), an area that has seen limited numerical exploration so far. Specifically, we construct an operational derivative matrix based on specialized generalized Jacobi polynomials, enabling a spectral collocation approach that is both accurate and computationally efficient. To the best of our knowledge, this work represents the first numerical methodology tailored specifically to such systems, filling a notable gap in the current literature. The proposed method offers a powerful combination of theoretical rigor and practical efficiency by leveraging the

ETNA
Kent State University and
Johann Radon Institute (RICAM)

intrinsic strengths of spectral collocation methods, including their superior convergence rates and capability to capture global solution behavior with high accuracy. A key innovation lies in the use of structured operational matrices, whose elements are explicitly computable, making the approach highly suitable for large-scale implementation. These matrices not only reduce the computational burden but also facilitate straightforward coding. Furthermore, the paper provides a detailed theoretical analysis, including the derivation of exact solutions in special cases and a rigorous convergence analysis. This firmly establishes our method as a pioneering and effective framework for advancing the numerical analysis of systems of DOFDEs (1.1).

The remainder of this paper is organized as follows. Section 2 introduces essential preliminaries, including definitions of fractional derivatives, Jacobi polynomials, and a discussion of their approximation capabilities. The Gauss–Jacobi quadrature formula is also presented to facilitate numerical integration. In Section 3, we derive the analytical solution of the underlying equation (1.1). Section 4 outlines the development of an efficient collocation-based numerical scheme tailored to equation (1.1). The convergence properties of the proposed method are rigorously analyzed in Section 5. Numerical experiments validating the accuracy and efficiency of the approach are provided in Section 6. Finally, Section 7 concludes the paper with a summary of the findings and a discussion of potential directions for future research.

2. Preliminaries and notation. In this section, we present the fundamental mathematical tools and formulations underpinning the proposed numerical approach. First, to facilitate an efficient collocation strategy, we utilize the shifted Jacobi polynomials, whose zeros serve as collocation nodes due to their optimal distribution and numerical stability. Moreover, the generalized Jacobi polynomials are introduced and adopted as basis functions for the construction of the approximate solution, taking advantage of their strong approximation capabilities.

2.1. Shifted Jacobi polynomials. Shifted Jacobi polynomials constitute a class of orthogonal polynomials defined on the interval $[0, T]$, obtained by applying the affine transformation $x = \frac{2t}{T} - 1$ to the classical Jacobi polynomials $J_n^{(\lambda,\mu)}(x)$, originally defined on $[-1, 1]$ [24]. The resulting family, denoted by $\hat{J}_{n,T}^{(\lambda,\mu)}(t) = J_n^{(\lambda,\mu)}\left(\frac{2t}{T} - 1\right)$, preserves orthogonality with respect to the shifted weight function $w_T^{(\lambda,\mu)}(t) = t^\mu(T - t)^\lambda$, with $\lambda, \mu > -1$. These polynomials also play a key role in interpolation schemes. Specifically, the shifted Jacobi interpolation operator $I_{N,T}^{(\lambda,\mu)}$ is defined by

$$I_{N,T}^{(\lambda,\mu)} f(t) = \sum_{j=0}^{N} \hat{f}_j \, \hat{J}_{j,T}^{(\lambda,\mu)}(t), \qquad \hat{f}_j = \frac{\langle f, \hat{J}_{j,T}^{(\lambda,\mu)} \rangle_{N, w_T^{(\lambda,\mu)}}}{\| \hat{J}_{j,T}^{(\lambda,\mu)} \|^2_{w_T^{(\lambda,\mu)}}},$$

where $\| \cdot \|_{w_T^{(\lambda,\mu)}}$ is the norm associated with the weighted L^2-space on $[0, T]$ and $\langle \cdot, \cdot \rangle_{N, w_T^{(\lambda,\mu)}}$ denotes the discrete inner product associated with the shifted Gauss–Jacobi quadrature rule

$$\langle f, g \rangle_{N, w_T^{(\lambda,\mu)}} = \sum_{j=0}^{N} f\left(s_{j,T}^{(\lambda,\mu)}\right) g\left(s_{j,T}^{(\lambda,\mu)}\right) \sigma_{j,T}^{(\lambda,\mu)},$$

which provides a powerful approximation of the well-known continuous inner product $(\cdot, \cdot)_{w_T^{(\lambda,\mu)}}$. Here, $\{s_{j,T}^{(\lambda,\mu)}, \sigma_{j,T}^{(\lambda,\mu)}\}_{j=0}^{N}$ represent the nodes and weights of the shifted Gauss–Jacobi quadrature on $[0, T]$. In the special case where $\lambda = \mu = 0$, corresponding to the shifted Legendre polynomials, error estimates for the interpolation and Gauss–Legendre quadrature

ETNA
Kent State University and
Johann Radon Institute (RICAM)

are given in [5]:

$$\begin{aligned} \|f - I_{N,T}^{(0,0)} f\|_{w_T^{(0,0)}} &\le CN^{-k} \|\partial_t^k f\|_{w_T^{(k,k)}}, \\ \left|(f,g)_{w_T^{(0,0)}} - \langle f,g\rangle_{N,w_T^{(0,0)}}\right| &\le CN^{-k} \|\partial_t^k f\|_{w_T^{(k,k)}} \|g\|_{w_T^{(0,0)}}, \qquad g \in \mathcal{P}_N, \end{aligned} \tag{2.1}$$

where $\mathcal{P}_N$ denotes the space of all polynomials of degree at most N and the parameter $k \in \mathbb{N}$ is the largest integer for which the weighted norm on the right-hand side of (2.1) remains finite.

2.2. Generalized Jacobi polynomials. To extend the applicability of Jacobi polynomials to broader classes of weight parameters, the shifted generalized Jacobi polynomials on Ω are introduced. For any integer values $\lambda, \mu \in \mathbb{Z}$, they are defined as

$$\mathcal{J}_n^{(\lambda,\mu)}(t) = 2^{\tilde{\lambda}+\tilde{\mu}}(1-t)^{\tilde{\lambda}} t^{\tilde{\mu}} J_{\tilde{n},1}^{(\hat{\lambda},\hat{\mu})}(t), \qquad \tilde{n} = n - (\tilde{\lambda} + \tilde{\mu}),$$

where

$$\tilde{\lambda} = \begin{cases} -\lambda & \lambda \le -1, \\ 0 & \lambda > -1, \end{cases} \qquad \hat{\lambda} = \begin{cases} -\lambda & \lambda \le -1, \\ \lambda & \lambda > -1, \end{cases}$$

and similarly for $\tilde{\mu}$ and $\hat{\mu}$. These generalized polynomials eliminate the classical restriction $\lambda, \mu > -1$ while retaining orthogonality with respect to the weight function $w_1^{(\lambda,\mu)}(t)$ [8]. Of particular significance is their vanishing behavior at the boundaries, which for $\lambda, \mu \le 0$ takes the form

$$\begin{aligned} \partial_t^j \mathcal{J}_n^{(\lambda,\mu)}(0) &= 0, \qquad j = 0, 1, \ldots, \tilde{\mu} - 1, \\ \partial_t^j \mathcal{J}_n^{(\lambda,\mu)}(1) &= 0, \qquad j = 0, 1, \ldots, \hat{\lambda} - 1. \end{aligned}$$

This boundary vanishing property makes them particularly suitable for use as basis functions in Galerkin and Petrov–Galerkin methods designed for functional problems with homogeneous Dirichlet boundary conditions.

3. Analytic representation and smoothness results. A fundamental objective of this section is to provide an analytic representation of the solution of equation (1.1) and to investigate its smoothness properties. It is easily verified that, using the coordinate transformation

$$V(t) = U(t) - \sum_{j=0}^{m-1} \frac{t^j}{j!} U_0^{(j)} \tag{3.1}$$

and the relation

$$D^\nu t^j = \begin{cases} 0 & j < \lceil \nu \rceil, \quad j \in \mathbb{N}, \\ \frac{\Gamma(j+1)}{\Gamma(j+1-\nu)} t^{j-\nu} & j \ge \lceil \nu \rceil, \end{cases}$$

the equation (1.1) is transformed into the following homogeneous initial value problem:

$$\int_0^m \omega(\nu) D^\nu V(t) d\nu = AV(t) + \tilde{F}(t), \tag{3.2}$$

ETNA
Kent State University and
Johann Radon Institute (RICAM)

where

$$\tilde{F}(t) = F(t) + A\sum_{j=0}^{m-1}\frac{t^j}{j!}U_0^{(j)} - \int_0^m \omega(\nu)\sum_{j=\lceil\nu\rceil}^{m-1}\frac{U_0^{(j)}}{\Gamma(j-\nu+1)}t^{j-\nu}d\nu. \tag{3.3}$$

By applying the Laplace transform to (3.2) and incorporating the homogeneous initial condition along with the auxiliary relation

$$\mathcal{L}[D^\nu V(t)] = s^\nu V(s) - \sum_{j=0}^{\lceil\nu\rceil-1} s^{\nu-j-1}V^{(j)}(0), \qquad V(s) = \mathcal{L}[V(t)],$$

we obtain the following expression:

$$\int_0^m \omega(\nu)s^\nu V(s)d\nu = AV(s) + \tilde{F}(s).$$

Defining $Q_m(s) = \int_0^m \omega(\nu)s^\nu d\nu$, the above relation can be written as

$$[Q_m(s)I - A]V(s) = \tilde{F}(s), \tag{3.4}$$

where I is the identity matrix. Assuming $\det(Q_m(s)I - A) \neq 0$, for all $s > 0$, the expression (3.4) simplifies to

$$V(s) = \big[Q_m(s)I - A\big]^{-1}\tilde{F}(s), \tag{3.5}$$

and thereby, taking the inverse Laplace transform of both sides of (3.5) yields

$$V(t) = \tilde{F}(t) * \mathcal{L}^{-1}\left[\big(Q_m(s)I - A\big)^{-1}\right], \tag{3.6}$$

where $*$ denotes the standard convolution operator.

Finally, by invoking the same procedure as in [22, Section 3], we establish that the inverse Laplace transform term $\mathcal{L}^{-1}\left[\big(Q_m(s)I - A\big)^{-1}\right]$ yields a bounded function. Consequently, the representation (3.6) along with (3.1) provides an analytic representation of the exact solution. Based on the above analysis and intermediate results, we are now in a position to formally state the following theorem for the problem under consideration:

THEOREM 3.1. *Assume* $\det(Q_m(s)I - A) \neq 0$, *for all* $s > 0$. *Then the analytic solution of equation* (1.1) *is represented by* (3.6) *and* (3.1).

To complete our analysis, we now turn our attention to the smoothness properties of the solution. Understanding the regularity of the solution not only provides deeper insight into the behavior of the system but also plays a crucial role in the development and analysis of numerical methods. To do this, using (3.5) and the relation

$$\mathcal{L}[V^{(k)}] = s^k\mathcal{L}[V] - \sum_{j=0}^{k-1} s^{k-j-1}V^{(j)}(0), \qquad k = 0, 1, \ldots, m,$$

we can conclude

$$\mathcal{L}[V^{(k)}] = \big(Q_m(s)I - A\big)^{-1}s^k\tilde{F}(s), \qquad k = 0, 1, \ldots, m. \tag{3.7}$$

ETNA
Kent State University and
Johann Radon Institute (RICAM)

Taking the inverse Laplace transform of both sides of (3.7) yields

$$V^{(k)}(t) = \tilde{F}(t) * \mathcal{L}^{-1}\left[s^k\right] * \mathcal{L}^{-1}\left[\left(Q_m(s)I - A\right)^{-1}\right].$$

Since $\mathcal{L}^{-1}\left[s^k\right] = \delta^{(k)}(t)$, where $\delta^{(k)}(t)$ denotes the k-th derivative of the Dirac delta function, and using the relation $\tilde{F}(t) * \delta^{(k)}(t) = (-1)^k \tilde{F}^{(k)}(t)$, we have

$$V^{(k)}(t) = (-1)^k \tilde{F}^{(k)}(t) * \mathcal{L}^{-1}\left[\left(Q_m(s)I - A\right)^{-1}\right], \qquad k = 0, 1, \ldots, m.$$

Consequently, the regularity of the exact solution depends directly on the smoothness properties of the known function $\tilde{F}$ in (3.3), as the solution inherits its differentiability from $\tilde{F}$.

4. Operational Jacobi collocation approach. As demonstrated in the preceding section, deriving an explicit analytical solution of the underlying problem is highly nontrivial and, in most cases, infeasible. This complexity necessitates the development of robust numerical techniques. In this section we formulate the operational spectral collocation method tailored to the linear system of DOFDEs given in (1.1). The distributed derivative is discretized using a shifted Gauss–Legendre quadrature rule on the interval $[0, m]$, leading to a fractional differential equation composed of multiple fractional-order terms. Subsequently, the unknown solution vectors are computed by employing a powerful collocation approach based on a family of special generalized Jacobi polynomials as basis functions and Gauss–Jacobi points as collocation nodes. To achieve this, by utilizing the shifted Gauss–Legendre quadrature rule on $[0, m]$, equation (1.1) is transformed into the following system of multi-term fractional differential equations (FDEs):

$$\sum_{i=0}^{M} \sigma_{i,m}^{(0,0)}\, \omega\big(s_{i,m}^{(0,0)}\big) D^{s_{i,m}^{(0,0)}} U(t) = AU(t) + F(t). \tag{4.1}$$

The collocation approximation $u_j^N(t)$ for $u_j(t)$ is defined by

$$u_j^N(t) = \sum_{i=m}^{N+m} b_{i-m}^j\, \mathcal{J}_i^{(0,-m)}(t) = \underline{b}^j\, \underline{\mathcal{J}}^{(0,-m)} = \underline{b}^j\, \mathcal{J}^{(0,-m)} \underline{T}, \qquad j = 1, 2, \ldots, n, \tag{4.2}$$

where $\underline{b}^j = [b_0^j, b_1^j, \ldots, b_N^j]$, $\underline{T} = [t^m, t^{m+1}, \ldots, t^{N+m}]^T$ and where

$$\underline{\mathcal{J}}^{(0,-m)} = \left[\mathcal{J}_m^{(0,-m)}(t),\ \mathcal{J}_{m+1}^{(0,-m)}(t),\ \ldots,\ \mathcal{J}_{N+m}^{(0,-m)}(t)\right]^T$$

is the vector of the generalized Jacobi polynomial basis. Also, $\mathcal{J}^{(0,-m)}$ is a lower-triangular generalized Jacobi coefficient matrix of order $N+1$. Inserting (4.2) into the k-th component of (4.1) yields

$$\begin{aligned} &\underline{b}^k\, \mathcal{J}^{(0,-m)} \sum_{i=0}^{M} \sigma_{i,m}^{(0,0)}\, \omega\big(s_{i,m}^{(0,0)}\big) D^{s_{i,m}^{(0,0)}} \underline{T} \\ &\quad = \sum_{j=1}^{n} a_{kj} \underline{b}^j\, \mathcal{J}^{(0,-m)} \underline{T} + f_k(t), \qquad k = 1, 2, \ldots, n. \end{aligned} \tag{4.3}$$

Using the relation $D^{s_{i,m}^{(0,0)}} t^j = \dfrac{j!}{\Gamma\big(j - s_{i,m}^{(0,0)} + 1\big)}$, valid for $j \geq m$, we obtain

$$D^{s_{i,m}^{(0,0)}} \underline{T} = \underline{T}^{m,i}, \tag{4.4}$$

ETNA
Kent State University and
Johann Radon Institute (RICAM)

where the j-th component is given by

$$\left[\underline{T}^{m,i}\right]_j = \frac{(m+j)!}{\Gamma\left(m+j-s_{i,m}^{(0,0)}+1\right)}\, t^{\,m+j-s_{i,m}^{(0,0)}}, \qquad j=0,1,2,\ldots$$

Substituting (4.4) into (4.3) gives

$$\begin{aligned} &\underline{b}^k \mathcal{J}^{(0,-m)} \sum_{i=0}^{M} \sigma_{i,m}^{(0,0)}\, \omega\left(s_{i,m}^{(0,0)}\right) \underline{T}^{m,i} \\ &\quad = \sum_{j=1}^{n} a_{kj} \underline{b}^j \mathcal{J}^{(0,-m)} \underline{T} + f_k(t), \qquad k=1,2,\ldots,n. \end{aligned} \tag{4.5}$$

To determine the unknown vectors $\{\underline{b}^k\}_{k=1}^n$, we evaluate both sides of (4.5) at the shifted Gauss–Legendre collocation points $\{s_{l,1}^{(0,0)}\}_{l=0}^N$ on Ω:

$$\underline{b}^k \mathcal{J}^{(0,-m)} \sum_{i=0}^{M} \sigma_{i,m}^{(0,0)}\, \omega\left(s_{i,m}^{(0,0)}\right) \underline{T}^{m,i}\left(s_{l,1}^{(0,0)}\right) = \sum_{j=1}^{n} a_{kj} \underline{b}^j \mathcal{J}^{(0,-m)} \underline{T}\left(s_{l,1}^{(0,0)}\right) + f_k\left(s_{l,1}^{(0,0)}\right),$$

for $k=1,2,\ldots,n$ and $l=0,1,\ldots,N$. The above system of algebraic equations can be written in a more compact form as

$$\begin{aligned} &\underline{b}^k \mathcal{J}^{(0,-m)} \sum_{i=0}^{M} \sigma_{i,m}^{(0,m)}\, \omega\left(s_{i,m}^{(0,0)}\right) \underline{TS}^{m,i} \\ &\quad = \sum_{j=1}^{n} a_{kj} \underline{b}^j \mathcal{J}^{(0,-m)} \underline{TS} + \underline{f_k S}, \qquad k=1,2,\ldots,n, \end{aligned} \tag{4.6}$$

where

$$\begin{aligned} \underline{TS}^{m,i} &= \left[\underline{T}^{m,i}(s_{0,1}^{(0,0)}),\ \underline{T}^{m,i}(s_{1,1}^{(0,0)}),\ \ldots,\ \underline{T}^{m,i}(s_{N,1}^{(0,0)})\right], \\ \underline{TS} &= \left[\underline{T}(s_{0,1}^{(0,0)}),\ \underline{T}(s_{1,1}^{(0,0)}),\ \ldots,\ \underline{T}(s_{N,1}^{(0,0)})\right], \\ \underline{f_k S} &= \left[f_k(s_{0,1}^{(0,0)}),\ f_k(s_{1,1}^{(0,0)}),\ \ldots,\ f_k(s_{N,1}^{(0,0)})\right]. \end{aligned}$$

The system (4.6) can be expressed compactly as

$$\underline{b} \bigotimes \mathcal{J}^{(0,-m)} \sum_{i=0}^{M} \sigma_{i,m}^{(0,0)}\, \omega\left(s_{i,m}^{(0,0)}\right) \underline{TS}^{m,i} = A\left[\underline{b} \bigotimes \mathcal{J}^{(0,-m)} \underline{TS}\right] + \underline{FS}, \tag{4.7}$$

where $\bigotimes$ denotes the tensor product,

$$\underline{b} = [\underline{b}^1, \underline{b}^2, \ldots, \underline{b}^n]^T, \qquad \text{and} \qquad \underline{FS} = [\underline{f_1 S}, \underline{f_2 S}, \ldots, \underline{f_n S}]^T.$$

Finally, the linear system of algebraic equations (4.7) (of order $n(N+1)$) can be written in the compact form

$$\Pi\, \underline{b} = \underline{FS}, \tag{4.8}$$

where Π is the system matrix. Solving (5.2) determines the unknown coefficients $\underline{b}$.

ETNA
Kent State University and
Johann Radon Institute (RICAM)

5. Convergence analysis. This section is devoted to a rigorous analysis of the convergence properties of the proposed method, with particular emphasis on the derivation of error bounds. To this end, we establish the following theorem, which precisely characterizes the error behavior of the collocation scheme:

THEOREM 5.1. *Let $\{u_j^N(t)\}_{j=1}^n$ denote the collocation approximations of the exact solutions $\{u_j(t)\}_{j=1}^n$ as defined in (4.2). Then, for each $j = 1, 2, \ldots, n$, the error satisfies the following estimate:*

$$\|u_j(t) - u_j^N(t)\|_{w_1^{(0,0)}} \leq C\, N^{-\psi},$$

where C is a positive finite constant independent of N and $\psi = \min\{p, k\}$. Here, p and k are the largest integers for which the following norms remain finite:

$$\|\partial_\nu^p\big(\omega(\nu)D^\nu u_j\big)\|_{w_m^{(p,p)}}, \qquad \|\partial_t^k f_j\|_{w_1^{(k,k)}}, \qquad \|\partial_t^k D^{s_{i,m}^{(0,0)}} u_j\|_{w_1^{(k,k)}},$$

for $i = 0, 1, \ldots, M$ and $j = 1, 2, \ldots, n$.

Proof. Building upon the framework developed in the preceding section, the linear algebraic system (4.8) can be equivalently reformulated in terms of the following operator representation:

$$\sum_{i=0}^{M} \sigma_{i,m}^{(0,0)}\, \omega\big(s_{i,m}^{(0,0)}\big) I_{N,1}^{(0,0)}\big(D^{s_{i,m}^{(0,0)}} U^N\big) = AU^N + I_{N,1}^{(0,0)} F, \tag{5.1}$$

where $U^N(t) = [u_j^N(t)]_{j=1}^n$ denotes the vector of collocation approximations of the exact solution $U(t)$ as defined in (4.2). Subtracting (5.1) from (1.1) results in

$$\int_0^m \omega(\nu) D^\nu U(t)\, d\nu - \sum_{i=0}^{M} \sigma_{i,m}^{(0,0)}\, \omega\big(s_{i,m}^{(0,0)}\big) I_{N,1}^{(0,0)}\big(D^{s_{i,m}^{(0,0)}} U^N\big) = AE_N + e_{I_{N,1}^{(0,0)}} F,$$

where $E_N(t) = U(t) - U^N(t)$ and $e_{I_{N,1}^{(0,0)}} F = F - I_{N,1}^{(0,0)} F$ denotes the interpolation error. This relation can be recast into the following form through straightforward algebraic manipulations:

$$\begin{aligned}\sum_{i=0}^{M} \sigma_{i,m}^{(0,0)}\, \omega\big(s_{i,m}^{(0,0)}\big) D^{s_{i,m}^{(0,0)}} E_N = {} & AE_N + e_{I_{N,1}^{(0,0)}} F - \mathrm{ELG}_{N,m}\big(\omega(\nu)D^\nu U\big) \\ & - \sum_{i=0}^{M} \sigma_{i,m}^{(0,0)}\, \omega\big(s_{i,m}^{(0,0)}\big) e_{I_{N,1}^{(0,0)}}\big(D^{s_{i,m}^{(0,0)}} U^N\big),\end{aligned} \tag{5.2}$$

where $\mathrm{ELG}_{N,m}(\cdot)$ denotes the error function resulting from discretizing the distributed-order fractional operator using an $(N+1)$-point Gauss–Legendre quadrature on $[0, m]$. Thus, applying the fractional integral operator $I^{s_{M,m}^{(0,0)}}$ to both sides of (5.2) yields

$$\begin{aligned}E_N(t) = \frac{1}{\sigma_{M,m}^{(0,0)}\, \omega\big(s_{M,m}^{(0,0)}\big)} \Bigg\{ & - \sum_{i=0}^{M-1} \sigma_{i,m}^{(0,0)}\, \omega\big(s_{i,m}^{(0,0)}\big) I^{s_{M,m}^{(0,0)} - s_{i,m}^{(0,0)}} E_N \\ & + AI^{s_{M,m}^{(0,0)}} E_N + I^{s_{M,m}^{(0,0)}} \Phi_N \Bigg\},\end{aligned} \tag{5.3}$$

ETNA
Kent State University and
Johann Radon Institute (RICAM)

where

$$\Phi_N = e_{I_{N,1}^{(0,0)}} F - \mathrm{ELG}_{N,m}\big(\omega(\nu) D^{\nu} U\big) - \sum_{i=0}^{M} \sigma_{i,m}^{(0,0)}\, \omega\big(s_{i,m}^{(0,0)}\big)\, e_{I_{N,1}^{(0,0)}}\big(D^{s_{i,m}^{(0,0)}} U^N\big).$$

It is easy to see that equation (5.3) can be represented as follows:

$$|E_N| \le C_1 \left\{ \sum_{i=0}^{M-1} I^{s_{M,m}^{(0,0)} - s_{i,m}^{(0,0)}} |E_N| + I^{s_{M,m}^{(0,0)}} |E_N| \right\} + \frac{1}{\big|\sigma_{M,m}^{(0,0)}\, \omega(s_{M,m}^{(0,0)})\big|} I^{s_{M,m}^{(0,0)}} |\Phi_N|, \tag{5.4}$$

where

$$C_1 = \frac{\max\big\{|\sigma_{i,m}^{(0,0)}\, \omega(s_{i,m}^{(0,0)})|,\ \|A\|_\infty\big\}}{\big|\sigma_{M,m}^{(0,0)}\, \omega(s_{M,m}^{(0,0)})\big|}, \qquad \text{for } i = 0, 1, \ldots, M-1.$$

Based on the definition of the fractional integral operator, the inequality (5.4) can be reformulated as

$$|E_N| \le C_1 \|K\|_\infty I^{\gamma} |E_N| + \frac{1}{\big|\sigma_{M,m}^{(0,0)}\, \omega(s_{M,m}^{(0,0)})\big|} I^{s_{M,m}^{(0,0)}} |\Phi_N|,$$

where $\gamma = \min_{0 \le i \le M-1}\big\{s_{M,m}^{(0,0)} - s_{i,m}^{(0,0)}\big\}$ and

$$K(t,s) = \Gamma(\gamma) \left(\sum_{i=0}^{M-1} \frac{(t-s)^{s_{M,m}^{(0,0)} - s_{i,m}^{(0,0)}}}{\Gamma\big(s_{M,m}^{(0,0)} - s_{i,m}^{(0,0)}\big)} + \frac{(t-s)^{s_{M,m}^{(0,0)} - \gamma}}{\Gamma\big(s_{M,m}^{(0,0)}\big)} \right)$$

is a continuous function on Ω. Applying Gronwall's inequality and using the boundedness of the operator $I^{s_{M,m}^{(0,0)}}$, we obtain

$$\|E_N\|_{w_1^{(0,0)}} \le C \|\Phi_N\|_{w_1^{(0,0)}},$$

and consequently, for $j = 1, 2, \ldots, n$, we have

$$\|u_j(t) - u_j^N(t)\|_{w_1^{(0,0)}} \le C \Bigg(\|e_{I_{N,1}^{(0,0)}} f_j\|_{w_1^{(0,0)}} + \big|\mathrm{ELG}_{N,m}\big(\omega(\nu) D^{\nu} u_j\big)\big| + \sum_{i=0}^{M} \big|\sigma_{i,m}^{(0,0)}\, \omega(s_{i,m}^{(0,0)})\big|\, \|e_{I_{N,1}^{(0,0)}}\big(D^{s_{i,m}^{(0,0)}} u_j\big)\|_{w_1^{(0,0)}} \Bigg). \qquad \square$$

Clearly, the desired result can be demonstrated by utilizing the inequalities (2.1).

REMARK 5.2. The convergence estimate in Theorem 5.1 provides a worst-case upper bound. The constants involved are chosen conservatively to ensure the estimate holds for all functions with the given regularity. In practice, for smooth or analytic test functions, the actual convergence is typically much faster (often exponential) than the algebraic rate predicted by the theorem. This is a well-known phenomenon in spectral methods and does not diminish the validity or usefulness of the theoretical analysis.

ETNA
Kent State University and
Johann Radon Institute (RICAM)

6. Illustrative examples. To demonstrate the accuracy and efficiency of the proposed spectral collocation method, three representative test problems are presented in this section. For each example, we compute the L^2-norm errors of the approximate solutions, which serve as a quantitative measure of the approximation accuracy. All numerical experiments were carried out using Wolfram Mathematica on a personal computing system equipped with a 13th-generation Intel ® Core™ i3-1315U processor (1.20 GHz), 20 GB of RAM, and a 64-bit architecture. This hardware configuration provided sufficient computational precision and performance for the considered numerical tasks. Additionally, all linear systems are solved using the `LinearSolve` function in Wolfram Mathematica, which implements an LU decomposition with partial pivoting to ensure numerical stability.

EXAMPLE 6.1. Consider the system

$$\begin{cases} \displaystyle\int_0^3 \Gamma(5-\nu) D^{\nu} U(t) d\nu = AU(t) + F(t), \\ U^{(j)}(0) = [0,0]^T, \qquad j = 0,1,2, \end{cases} \tag{6.1}$$

where

$$A = \begin{bmatrix} 1 & 1 \\ 1 & -1 \end{bmatrix}, \qquad F(t) = \begin{bmatrix} \frac{6t^2-6}{ln(t)} - t^3 - t^4 \\ \frac{24t(t^3-1)}{ln(t)} - t^3 + t^4 \end{bmatrix}, \qquad U(t) = \begin{bmatrix} t^3 \\ t^4 \end{bmatrix}.$$

The illustrative example (6.1) is solved using the proposed method, and the corresponding results are presented in Tables 6.1–6.3 and Figure 6.1. These findings highlight both the robustness and the high efficiency of the adopted approach. Indeed, Theorem 5.1 establishes the algebraic error estimate $\|u_j(t) - u_j^N(t)\|_{w_1^{(0,0)}} \leq CN^{-\psi}$ for our spectral method, where ψ is the convergence rate determined by the regularity of the solution. To validate this theoretical result, we compare the computed numerical errors with the predicted bound for various values of N. Tables 6.1 and 6.2 summarize this comparison. The constant C is estimated from the numerical results as $C = \max_N \|u_j(t) - u_j^N(t)\|_{w_1^{(0,0)}} N^{\psi}$, ensuring that the bound holds for all tested cases. As clearly observed, the inequality $\|u_j(t) - u_j^N(t)\|_{w_1^{(0,0)}} \leq CN^{-\psi}$ is satisfied for various approximation degrees N, confirming the reliability of the theoretical estimate. Nevertheless, the theoretical bound in Theorem 5.1 is not sharp. This is expected because the theoretical analysis employs worst-case estimates to ensure generality, while the numerical examples involve smooth test functions. More precisely, in all numerical tests, the observed errors are significantly smaller than the upper bound predicted by the theorem, which is expected because the theoretical analysis employs conservative constants to ensure generality. Furthermore, the rapid decay of the reported errors approaching zero even for relatively low approximation orders, combined with the linear behavior of the logarithm of the error depicted in Figure 6.1, provides clear evidence of the attainment of spectral accuracy.

To assess the conditioning of the coefficient matrix, we compute its condition number $\kappa(\Pi) = \|\Pi\| \, \|\Pi^{-1}\|$ for various values of N using the well-known Euclidean matrix norm. Table 6.3 presents the condition number for various N in comparison with the residual $\frac{\|\Pi b - FS\|}{\|FS\|}$. As observed, the condition number grows moderately with N but remains within acceptable bounds. This growth is expected due to the spectral nature of the basis functions and is consistent with observations in standard spectral methods [24]. Despite this growth, the residuals remain of the order of 10^{-24}, confirming that the linear systems are solved accurately.

6.1. Application to a practical problem. In the subsequent example, we turn our attention to a practical and physically motivated problem. The solar-wind-driven magnetosphere-ionosphere (WINDMI) system, which can be modeled as a complex driven-damped dynamical

ETNA
Kent State University and
Johann Radon Institute (RICAM)

TABLE 6.1
Numerical performance metrics for Example 6.1: L^2-error norms $\|u_1(t)-u_1^N(t)\|_{w_1^{(0,0)}}$ versus discretization parameter N, with convergence constant $C = 9.2 \times 10^{-4}$ and $\psi = 1$.

N	$\|u_1(t) - u_1^N(t)\|_{w_1^{(0,0)}}$	$CN^{-\psi}$
2	4.6×10^{-4}	4.6×10^{-4}
4	5.2×10^{-6}	2.3×10^{-4}
6	2.6×10^{-8}	1.5×10^{-4}
8	7.5×10^{-11}	1.1×10^{-4}
12	1.5×10^{-16}	7.6×10^{-5}
16	7.1×10^{-23}	5.7×10^{-5}

TABLE 6.2
Numerical performance metrics for Example 6.1: L^2-error norms $\|u_2(t)-u_2^N(t)\|_{w_1^{(0,0)}}$ versus discretization parameter N, with convergence constant $C = 0.0029$ and $\psi = 3$.

N	$\|u_2(t) - u_2^N(t)\|_{w_1^{(0,0)}}$	$CN^{-\psi}$
2	3.6×10^{-4}	3.6×10^{-4}
4	8.2×10^{-7}	4.5×10^{-5}
6	1.2×10^{-9}	1.3×10^{-5}
8	1.3×10^{-12}	5.7×10^{-6}
12	2.2×10^{-18}	1.7×10^{-6}
16	1.5×10^{-24}	7.1×10^{-7}

TABLE 6.3
Numerical performance metrics for the linear system solution of Example 6.1.

N	$\kappa(\Pi)$	$\frac{\|\Pi b - FS\|}{\|FS\|}$
2	2.26	2.29×10^{-24}
4	17.34	1.56×10^{-24}
6	84.7	1.24×10^{-24}
8	295.14	1.69×10^{-24}
12	1969.54	2.4×10^{-24}
16	8202.21	1.7×10^{-24}

system, is known to exhibit a rich spectrum of dynamical behaviors. These include stable low-level plasma convection, intermittent releases of plasma energy stored in the geotail and released into the ionosphere (commonly referred to as substorms), and extended intervals of sustained, high-magnitude unloading. This system provides a challenging test case for numerical methods due to its multiscale nature and sensitivity to perturbations. The classical integer-order WINDMI model is given in [22] by

$$\begin{aligned} \frac{du_1}{dt} &= u_2, \\ \frac{du_2}{dt} &= u_3, \\ \frac{du_3}{dt} &= -au_3 - u_2 + b - e^{u_1}, \end{aligned} \tag{6.2}$$

where u_1, u_2, and u_3 are the state variables of the system and a, b, and e are positive parameters governing the system's dynamics.

ETNA
Kent State University and
Johann Radon Institute (RICAM)

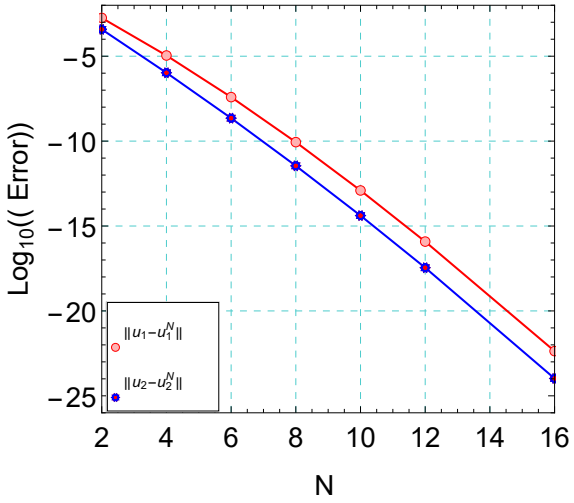

FIG. 6.1. *Semi-logarithmic plot of the numerical errors for Example 6.1 versus different N.*

In what follows, we extend this formulation by introducing the distributed-order counterpart of the WINDMI system (6.2), thereby enabling the investigation of its behavior within a broader and more flexible fractional-order framework. This extension allows us to capture a continuous spectrum of memory effects, which is particularly relevant for modeling complex multiscale phenomena in space-weather dynamics. Consequently, the distributed-order fractional extension of the WINDMI system (6.2) can be expressed as follows:

$$\begin{aligned}
&\int_0^1 \omega(\nu) D^\nu u_1(t) d\nu = u_2(t),\\
&\int_0^1 \omega(\nu) D^\nu u_2(t) d\nu = u_3(t),\\
&\int_0^1 \omega(\nu) D^\nu u_3(t) d\nu = -a u_3(t) - u_2(t) + b - e^{u_1(t)},\\
&u_1(0) = u_1^{(0)}, \qquad u_2(0) = u_2^{(0)}, \qquad u_3(0) = u_3^{(0)}.
\end{aligned}$$

Clearly, at the equilibrium point $\hat{U} = [ln(b), 0, 0]$, we have

$$\int_0^1 \omega(\nu) D^\nu \hat{U} d\nu = F(\hat{U}) = 0,$$

where $F = [u_2,\ u_3,\ \ -au_3 - u_2 + b - e^{u_1}]^T$. Therefore, by linearizing the function F and some simple manipulations, we deduce that the system's behavior in the vicinity of the equilibrium point $\hat{U}$ can be accurately approximated by the linear model

$$\int_0^1 \omega(\nu) D^\nu Y(t) d\nu = AY(t), \qquad Y(0) = U(0) - \hat{U}, \tag{6.3}$$

ETNA
Kent State University and
Johann Radon Institute (RICAM)

where $Y = U - \hat{U}$ and $A = (\frac{\partial F}{\partial U})|_{U=\hat{U}}$ is given by

$$A = \begin{bmatrix} 0 & 1 & 0 \\ 0 & 0 & 1 \\ -b & -1 & -a \end{bmatrix}.$$

EXAMPLE 6.2. Consider equation (6.3) with $a = 1, b = 2$, and $u_1^{(0)} = u_2^{(0)} = u_3^{(0)} = 0$. The above equation is solved by applying the variable transformation $\tilde{Y} = Y + \hat{U}$, which reformulates the problem into one with homogeneous initial conditions. The corresponding numerical results are presented in Table 6.4 and Figure 6.2. In the absence of an exact analytical solution, a reference solution obtained with $N = 60$ is employed for comparison, and the associated errors are evaluated accordingly. These outcomes clearly demonstrate the effectiveness of the proposed method in accurately approximating the solutions of this practical problem, even in the absence of an analytical benchmark. Unlike the previous synthetic examples, the WINDMI system exhibits a richer dynamical behavior and a wider frequency content. This intrinsic complexity limits the convergence rate. Nevertheless, the error decreases consistently, and the method remains stable for all tested N.

TABLE 6.4
Numerical performance metrics for Example 6.2: L^2-error norms versus discretization parameter N.

N	$\|u_1(t) - u_1^N(t)\|_{w_1^{(0,0)}}$	$\|u_2(t) - u_2^N(t)\|_{w_1^{(0,0)}}$	$\|u_3(t) - u_3^N(t)\|_{w_1^{(0,0)}}$
6	4.8×10^{-4}	6.7×10^{-4}	1.9×10^{-3}
12	1.3×10^{-4}	1.7×10^{-4}	4.1×10^{-4}
18	5.15×10^{-5}	7.3×10^{-5}	1.6×10^{-4}
24	2.8×10^{-5}	3.8×10^{-5}	8.3×10^{-5}
36	9.6×10^{-6}	1.3×10^{-5}	2.7×10^{-5}
48	2.9×10^{-6}	3.9×10^{-6}	9.2×10^{-6}

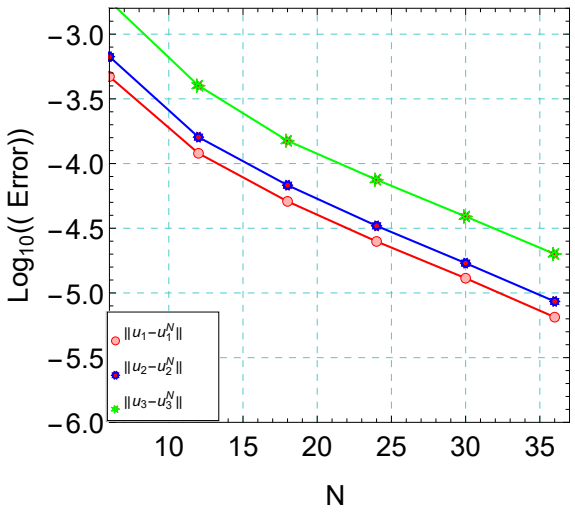

FIG. 6.2. *Semi-logarithmic plot of the numerical errors for Example 6.2 versus different N.*

ETNA
Kent State University and
Johann Radon Institute (RICAM)

7. Conclusion. In this study, we developed an operational Jacobi collocation framework for the numerical solution of linear systems of distributed-order fractional differential equations (DOFDEs). The proposed scheme, which combines high-order quadrature discretization with generalized Jacobi operational matrices, exhibits both spectral accuracy and computational efficiency. A rigorous convergence analysis confirms the theoretical error estimates, and numerical experiments, including a real-world application to the WINDMI system, validate the robustness and effectiveness of the method. These results highlight the capability of the proposed approach to capture complex distributed-order dynamics with high precision.

REFERENCES

[1] M. ABBASZADEH AND M. DEHGHAN, *An improved meshless method for solving two-dimensional distributed order time-fractional diffusion-wave equation with error estimate*, Numer. Algorithms, 75 (2017), pp. 173–211.

[2] ———, *Meshless upwind local radial basis function-finite difference technique to simulate the time-fractional distributed-order advection–diffusion equation*, Engineering Comput., 37 (2021), pp. 873–889.

[3] I. AHMAD, I. MEKAWY, M. N. KHAN, R. JAN, AND S. BOULAARAS, *Modeling anomalous transport in fractal porous media: a study of fractional diffusion PDEs using numerical method*, Nonlinear Engineering, 13 (2024), Paper No. 20220366, 11 pages.

[4] W. BU, L. JI, Y. TANG, AND J. ZHOU, *Space-time finite element method for the distributed-order time fractional reaction diffusion equations*, Appl. Numer. Math., 152 (2020), pp. 446–465.

[5] Y. CHEN AND T. TANG, *Spectral methods for weakly singular Volterra integral equations with smooth solutions*, J. Comput. Appl. Math., 233 (2009), pp. 938–950.

[6] K. DIETHELM AND N. J. FORD, *Analysis of fractional differential equations*, J. Math. Anal. Appl., 265 (2002), pp. 229–248.

[7] ———, *Numerical analysis for distributed-order differential equations*, J. Comput. Appl. Math., 225 (2009), pp. 96–104.

[8] A. FAGHIH AND P. MOKHTARY, *A novel Petrov-Galerkin method for a class of linear systems of fractional differential equations*, Appl. Numer. Math., 169 (2021), pp. 396–414.

[9] M. FARDI, *A kernel-based pseudo-spectral method for multi-term and distributed order time-fractional diffusion equations*, Numer. Methods Partial Differential Equations, 39 (2023), pp. 2630–2651.

[10] N. J. FORD, M. L. MORGADO, AND M. REBELO, *A numerical method for the distributed order time-fractional diffusion equation*, in ICFDA'14 International Conference on Fractional Differentiation and Its Applications, IEEE Conference Proceedings, Los Alamitos, 2014, pp. 1–6.

[11] F. GENG AND X. WU, *Kernel functions-based approach for distributed order diffusion equations*, Numer. Methods Partial Differential Equations, 37 (2021), pp. 1269–1281.

[12] S. IRANDOUST-PAKCHIN, M. H. DERAKHSHAN, S. REZAPOUR, AND M. ADEL, *An efficient numerical method for the distributed-order time-fractional diffusion equation with the error analysis and stability properties*, Math. Methods Appl. Sci., 48 (2025), pp. 2743–2765.

[13] J. JIANG, *The distributed order models to characterize the flow and heat transfer of viscoelastic fluid between coaxial cylinders*, Phys. Scripta, 99 (2024), Paper No. 015233, 16 pages.

[14] Y. JIANG AND H. G. SUN, *Flow and convection heat of spatial fractional derivative non-Newtonian fluids in fractal main channels*, IFAC-PapersOnLine, 58 (2024), pp. 386–389.

[15] C. V. D. KUMAR, D. G. PRAKASHA, P. VEERESHA, AND M. KAPOOR, *A homotopy-based computational scheme for two-dimensional fractional cable equation*, Mod. Phys. Lett. B, 38 (2024), Paper No. 2450292.

[16] S. KUMAR AND A. ATANGANA, *Numerical solution of ABC space-time fractional distributed order reaction-diffusion equation*, Numer. Methods Partial Differential Equations, 38 (2022), pp. 406–421.

[17] J. A. LE ROUX, *A tempered fractional kinetic transport theory for energetic particle interaction with quasi-two-dimensional turbulence in the large-scale solar wind*, Astrophysical J., 968 (2024), Paper No. 112, 22 pages.

[18] A. V. MILOVANOV AND J. J. RASMUSSEN, *Turbulence spreading by resonant wave-wave interactions: a fractional kinetics approach*, Phys. Rev. E, 109 (2024), Paper No. 045105, 18 pages.

[19] G. MONZÓN, *Fractional variational iteration method for higher-order fractional differential equations*, J. Fract. Calc. Appl., 15 (2024), Paper No. 4, 15 pages.

[20] S. PATNAIK AND F. SEMPERLOTTI, *Application of variable-and distributed-order fractional operators to the dynamic analysis of nonlinear oscillators*, Nonlinear Dynam., 100 (2020), pp. 561–580.

[21] W. QING, B. PAN, C. ZHU, AND Y. RAN, *Designing fractional homotopy methods for trajectory optimization from the smoothing perspective*, J. Guidance Control Dynam., 48 (2025), pp. 2599–2609.

ETNA
Kent State University and
Johann Radon Institute (RICAM)

[22] H. SABERI NAJAFI, A. REFAHI SHEIKHANI, AND A. ANSARI, *Stability analysis of distributed order fractional differential equations*, Abstr. Appl. Anal., 2011, Paper No. 175323, 12 pages.
[23] S. SABERMAHANI AND Y. ORDOKHANI, *Solving distributed-order fractional optimal control problems via the Fibonacci wavelet method*, J. Vib. Control, 30 (2024), pp. 418–432.
[24] J. SHEN, T. TANG, AND L.-L. WANG, *Spectral Methods*, Springer, Heidelberg, 2011.
[25] H. SOBHANI, A. AZIMI, A. NOGHREHABADI, AND M. MOZAFARIFARD, *Numerical study and parameters estimation of anomalous diffusion process in porous media based on variable-order time fractional dual-phase-lag model*, Numer. Heat Transfer, Part A: Applications, 83 (2023), pp. 679–710.
[26] N. H. SWEILAM, S. M. AHMED, AND S. M. AL-MEKHLAFI, *Two-dimensional distributed order cable equation with non-singular kernel: a nonstandard implicit compact finite difference approach*, J. Appl. Math. Comput. Mech., 23 (2024), pp. 93–104.
[27] H. B. YADETA AND S. SHAW, *Unsteady fractional dispersion under controlled targeted drug elimination and non-Newtonian rheology*, Nonlinear Dynam., 113 (2025), pp. 21181–21197.
[28] B. YUTTANAN AND M. RAZZAGHI, *Legendre wavelets approach for numerical solutions of distributed order fractional differential equations*, Appl. Math. Model., 70 (2019), pp. 350–364.
[29] A. ZHANG, R. M. GANJI, H. JAFARI, M. N. NCUBE, AND L. AGAMALIEVA, *Numerical solution of distributed order integro-differential equations*, Fractals, 30 (2022), Paper No. 2240123, 11 pages.
[30] A. ZHAO, J. LI, AND Y. LEI, *Distributed robust control for a class of semilinear fractional-order reaction–diffusion systems*, Nonlinear Dynam., 109 (2022), pp. 1743–1762.
[31] T. ZHAO, C. LI, AND D. LI, *Efficient spectral collocation method for fractional differential equation with Caputo-Hadamard derivative*, Fract. Calc. Appl. Anal., 26 (2023), pp. 2903–2927.